SURFACE AND INTERFACE ANALYSIS
Surf. Interface Anal. **30**, 396–400 (2000)

Study of the growth of ultrathin films of NiO on Cu(111)

M. Sánchez-Agudo,[1] F. Yubero,[2] G. G. Fuentes,[1] A. Gutiérrez,[3] M. Sacchi,[4] L. Soriano* and J. M. Sanz[1]

[1] Departamento de Física Aplicada C-XII, Instituto de Ciencia de Materiales Nicolás Cabrera, Universidad Autónoma de Madrid, Cantoblanco, E-28049 Madrid, Spain

[2] Instituto de Ciencia de Materiales de Sevilla, CSIC-Universidad de Sevilla, Av. Américo Vespucio s/n, Isla de la Cartuja, E-41092 Sevilla, Spain

[3] Departamento de Ciencia y Tecnología de Materiales, Universidad Miguel Hernández, Avda. Ferrocarril s/n, E-03202 Elche, Spain

[4] Laboratoire pour l'Utilization du Rayonement Electromagnetique (LURE), Université Paris-Sud, Bâtiment 209 d, F-91405 Orsay, France

We have studied the early stages of growth of the layers formed by Ni evaporation in an oxygen atmosphere at room temperature on a Cu(111) single crystal. The layers have been analysed by XPS and x-ray absorption spectroscopy as a function of the deposition time. A background analysis of the XPS spectra has also been performed. We have found a Stranski–Krastanov way of growth, i.e. the formation of a metallic Ni monolayer followed by the formation of defective NiO islands. Further deposition leads to the formation of stoichiometric NiO.

KEYWORDS: oxide/metal interface; growth; XPS

INTRODUCTION

The main purpose of this paper is the study of the early stages of growth of ultrathin films of NiO on Cu(111) at room temperature. The study of ultrathin oxide films on metal substrates and their interfaces has attracted much interest in recent years.[1–3] The interesting catalytic properties of NiO, as well as the potential use of magnetic NiO/CuO multilayers, support this work. The complex electronic structure of NiO has been widely studied for years.[4,5] The influence of surface defects on the electronic structure in defective NiO surfaces[6,7] and nanoparticles[8,9] has also been reported. Other related experiments include the growth of ultrathin films of NiO on different substrates (e.g. MgO,[10,11] V_2O_5,[12] HOPG[13]) as well as of different oxides (e.g. ZnO_x[14] and Fe_2O_3[15]) on Cu(111).

In this work, ultrathin NiO films have been grown by thermal evaporation of nickel in an oxygen atmosphere on a Cu(111) single crystal at room temperature. Substrate and overlayer have been analysed by means of x-ray photoelectron spectroscopy (XPS) and x-ray absorption spectroscopy (XAS) as a function of the deposition time. Firstly we present a chemical analysis based on the core-level XPS spectra. Then, a quantification of the background due to the inelastically scattered electrons has been performed following the formalism of Tougaard.[16,17] Finally, and taking advantage of the larger probing depth of XAS as compared with XPS, the chemical state of the Cu substrate for large coverages (some tens of monolayers) has also been analysed.

* Correspondence to: L. Soriano, Departamento de Física Aplicada C-XII, Instituto de Ciencia de Materiales Nicolás Cabrera, Universidad Autónoma de Madrid, Cantoblanco, E-28049 Madrid, Spain.
E-mail: l.soriano@uam.es

Contract/grant sponsor: DGICYT, Spain; Contract/grant number: PB96-0061.

Contract/grant sponsor: UE-TMR; Contract/grant number: ERBFMGECT 950063.

EXPERIMENTAL

Layers of NiO were deposited by evaporation of pure Ni (99.98% from Goodfellow) in an oxygen atmosphere at room temperature. Nickel was evaporated resistively at constant current from a tungsten filament surrounded by an Ni wire. Oxygen was introduced through a pipe directed towards the sample (2 cm) in order to obtain a higher oxygen pressure in the surroundings of the sample. The oxygen pressure, as measured in the ultrahigh vacuum (UHV) chamber, was maintained constant at 5×10^{-7} Torr. Previously, the Cu(111) single-crystal substrate was submitted to several cycles of Ar^+ sputtering and annealing at 700 °C until it appeared clean, as observed by XPS.

The XPS spectra were acquired in a PHI-3027 spectrometer equipped with an Mg Kα excitation source and a double-pass cylindrical mirror analyser (CMA) working at 20 eV pass energy and giving a full width at half-maximum (FWHM) of the Cu $2p_{3/2}$ photoelectron line of 1.8 eV. The experimental raw data were corrected by the transmission function of the electron energy analyser. Inelastic mean free paths of 9.8 and 8.3 Å were used to analyse the Ni 2p and Cu 2p peaks.[18]

The XAS measurements were performed at the SA8 beam-line of LURE using a double-crystal (Beryl) monochromator. The resolution was better than 0.4 eV at 930 eV. The spectra were taken in the total yield mode.

Received 15 July 1999
Revised 24 November 1999; Accepted 24 November 1999

The estimated mean probing depth of XAS is 40 Å.[19] The spectra were normalized to the incident current I_0. The energy scale was calibrated taking the maximum of the Cu 2p edge in CuO at 931.2 eV.[20]

RESULTS AND DISCUSSION

X-ray photoelectron spectroscopy chemical analysis

The photoemission spectra of O 1s (a) and Ni 2p (b) as a function of the evaporation time are shown in Fig. 1. The shape and energy position of the Ni 2p spectra change progressively upon deposition. The spectra have been divided into three different regions. In region (i), corresponding to very low coverages (3–19 min), the Ni $2p_{3/2}$ line is narrow and centred at 853.0 eV. These spectra agree in shape and energy position with that of metallic Ni.[21] On the contrary, the spectra of region (iii), corresponding to high coverages (404 min), agree very well with that reported for NiO.[7] The spectra of region (ii) (19–164 min) are rather complex but they can be fitted as a linear combination of those corresponding to metallic Ni and NiO, indicating the presence of both phases in the deposit.

With regard to the O 1s XPS spectra shown in Fig. 1(a), it is interesting to point out that in region (i) no oxygen species have been absorbed. On the contrary, for regions (ii) and (iii) we observe two peaks at 529.7 and 531.6 eV, respectively. The former can be assigned to oxygen in the NiO lattice,[10] whereas the latter is known to belong to oxygen absorbed on defective NiO.[13] The Cu 2p XPS spectra for regions (i) and (ii) are shown in Fig. 2. All these spectra are characterized by a narrow Cu $2p_{3/2}$ peak located at 932.9 eV binding energy that corresponds to metallic Cu. This assignment is also supported by the shape and energy position of the Cu Auger LMM peaks (not shown

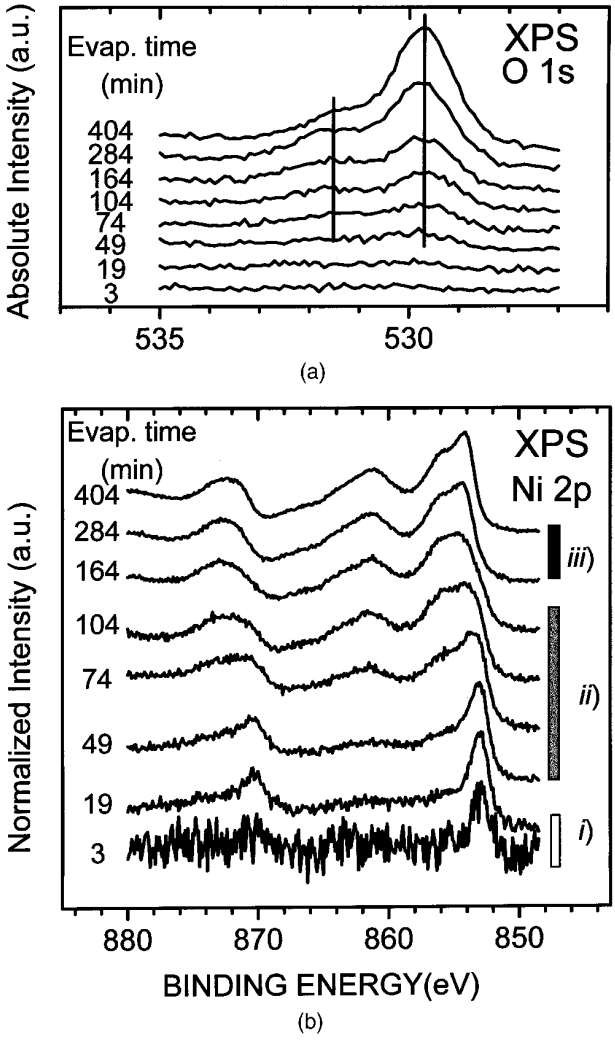

Figure 1. The XPS spectra of O 1s (a) and Ni 2p (b) as a function of the evaporation time. For explanation of regions (i), (ii) and (iii), see text.

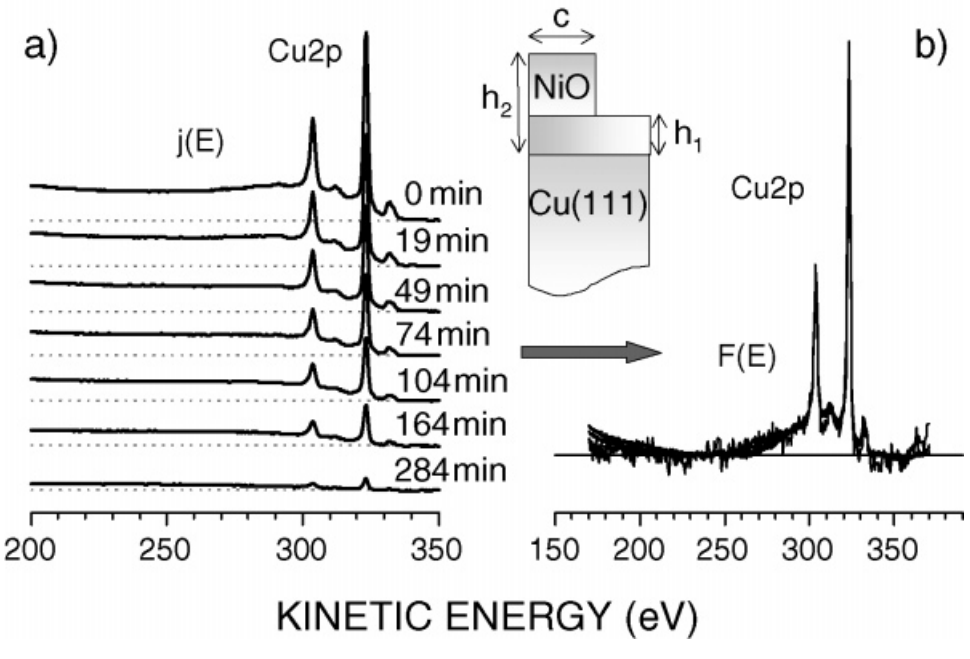

Figure 2. (a) Copper 2p XPS spectra as a function of the evaporation time. Horizontal lines indicate the extrapolated background. (b) The same spectra after inelastic background subtraction. The inset represents the profile and parameters used in the quantitative background analysis.

here). For evaporation time >284 min, the Cu 2p XPS signal could not be detected because the inelastic mean free path (IMFP) of the Cu 2p photoelectrons is much lower than the thickness of the deposit.

Three important conclusions can be inferred from the above results:

(1) In region (i), Ni and Cu atoms remain unoxidized. Furthermore, considering the well-known oxidation kinetics of Ni,[22] it seems that the presence of the Cu substrate hinders the oxidation of the deposited Ni atoms. In fact this effect has been observed previously in the Ni/Cu(100) system.[21]
(2) For region (ii), Ni atoms are partially oxidized leading to defective NiO, as revealed by the characteristic Ni 2p and O 1s spectra of the defective oxide shown in Ref. 13.
(3) For thicker overlayers, mainly stoichiometric NiO is formed.

X-ray photoelectron spectroscopy background analysis

Quantification of the photoemission spectra by inelastic peak shape analysis relies on a physical description of the electron transport processes.[23] This method has already been applied to study the growth mode of several thin films.[24–29] The description of the energy losses during electron transport out of the sample is done through the universal cross-section suggested by Tougaard,[23] i.e. in this case we have used $B = 3350$ eV^2 as determined from a correct background subtraction of the Cu 2p line from the clean Cu(111) substrate (see below).

The analysis procedure was performed by using the known QUASES© software according to the following steps. First, the contribution $j(E)$ of the photoelectrons coming from a core line was isolated. This is done by subtraction of a straight line that extrapolates the background in the high-kinetic-energy side of the peak [dotted line in Fig. 2(a)]. Then, the inelastic background is substracted in order to determine the background-corrected spectra $F(E)$. We have used the universal cross-section mentioned above. The shape of $F(E)$ gives the energy distribution of the originally excited electrons and its intensity is related to the number of emitting atoms in the analysed region of the sample. Two main constrains affect the determination of $F(E)$. First, the background in the low-kinetic-energy side of the peak, far from the position of the main (no-loss) line, must be zero. Second, $F(E)$ must be equal in shape and intensity to that obtained from a reference bulk sample of the same material. Figure 2(b) shows the set of background-corrected spectra $F(E)$. Note that the same originally excited spectrum $F(E)$ is obtained for all the analysed samples, which validates the analysis.

Quantitative analysis of the background indicates that the growth mode is of the Stranski–Krastanov type, i.e. completion of a full layer followed by growth of islands on top of that layer. The parameters describing the mode are the height h_1 of the initial layer completely covering the Cu surface, the height h_2 of the islands and the surface coverage c of these islands (see inset of Fig. 2). In Table 1 we have summarized the values obtained for these parameters. Determination of the height h_2 of the islands from the Cu 2p signals was not possible because of the short IMFP of the Cu 2p photoelectron peaks. However, a similar analysis was done for some of the corresponding Ni 2p peaks, whose IMFP is 20% higher than that of the Cu 2p peaks. The results were coherent with the profiles obtained from analysis of the Cu 2p peaks, with values for h_2 of ~30–40 Å.

Table 1. Parameters describing the growth mode of the samples depicted in Fig. 2

Sample	Height h_1 (Å)	Height h_2 (Å)	Coverage c (%)
0 min	0	0	—
19 min	2.7	0	0
49 min	3.8	>30	8
74 min	4.3	>30	20
104 min	5.0	>30	28
164 min	5.5	>30	44
284 min	10	>30	71

According to the background analysis, together with the information obtained from chemical analysis, the growth mechanism of the NiO layer on a clean Cu(111) substrate can be described by the following stages: formation of a homogeneous layer of ~3 Å (~1 ML) of metallic Ni completely covering the Cu(111) surface; and growth of aggregates of defective NiO ~30–40 Å thick, then a slow increase of the Ni layer thickness, partly oxidized to NiO, and simultaneous increase of the coverage with the defective NiO islands as described in Table 1. Note that the lateral size of the NiO aggregates is not available by this XPS background analysis. Finally, coalescence of the NiO aggregates occurs to form a stoichiometric NiO layer.

X-ray absorption spectroscopy chemical analysis

The Ni 2p XAS spectra for the same regions as in Fig. 1 are shown in Fig. 3. We have also included the spectra of metallic Ni and NiO as references. These spectra have already been interpreted in the literature.[8,30] Whereas the spectrum of metallic Ni is related to unoccupied d-bands,[30] the spectrum of NiO corresponds to atomic transitions in the Ni^{2+} high-spin configuration within an octahedral crystal field of 1.8 eV.[8] Both Ni and NiO XAS spectra show a main band centred at ~854 eV and a weaker one centred at ~872 eV arising from transitions from Ni $2p_{3/2}$ and $2p_{1/2}$ orbitals, respectively. The spectrum corresponding to region (i) reproduces rather well the spectrum of metallic Ni, in agreement with the XPS results. The spectra corresponding to region (ii) can be considered a linear combination of the spectra of Ni and NiO. In fact, the double peak at the Ni $2p_{1/2}$ band reveals the formation of the oxide, in agreement with the XPS data. Finally, the spectrum corresponding to region (iii) approaches that of NiO, although it is slightly broader, probably due to the formation of defective NiO as stated from the XPS spectra.

The corresponding Cu 2p XAS spectra are shown in Fig. 4. We have also included the spectrum of CuO for comparison. Both clean Cu and CuO reference spectra agree well with those reported in the literature.[20,31] It is clear that for regions (i) and (ii) the Cu substrate remains metallic, in agreement with the XPS analysis. However, the spectrum of region (iii) shows a narrow prepeak located at 931.2 eV. This is a clear indication that, at this

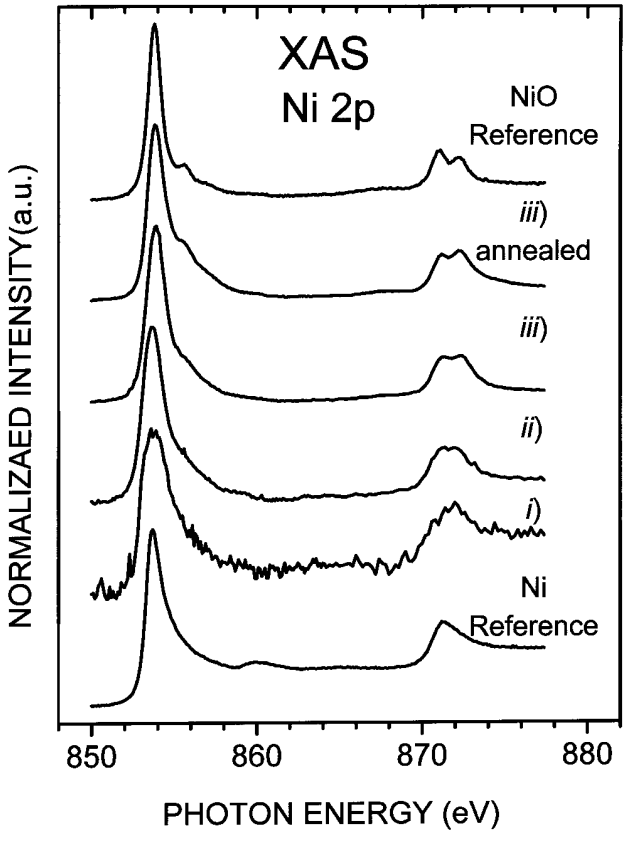

Figure 3. Nickel 2p XAS spectra for the same regions as the spectra in Fig. 1.

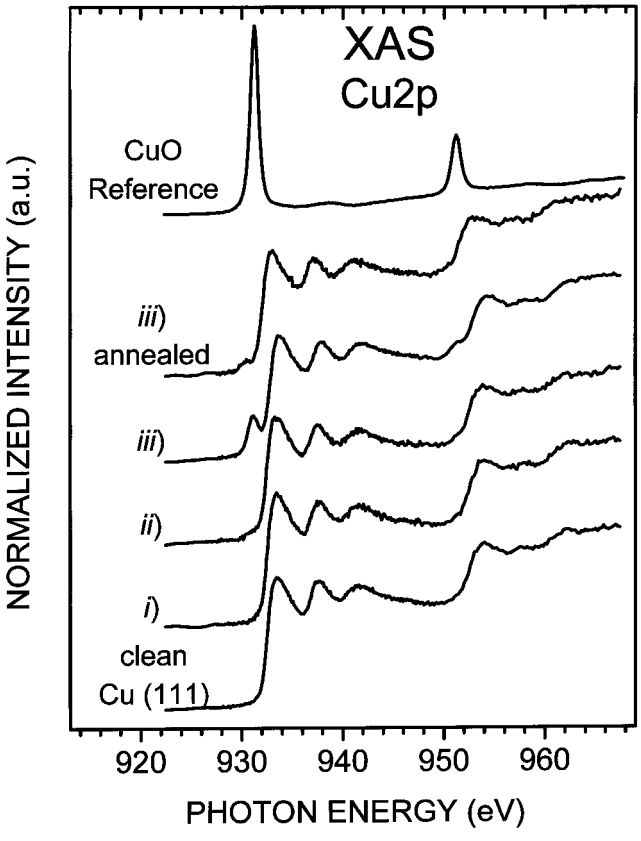

Figure 4. Copper 2p XAS spectra for the same regions as the spectra in Fig. 1.

stage of the NiO film growth, the substrate is oxidized to CuO at the interface (cf. CuO reference spectrum at the top of Fig. 4). After this stage, the film was annealed at 400 °C in an oxygen atmosphere of 8×10^{-6} Torr. Surprisingly, the CuO formed at the interface almost disappears (see the spectra labelled as region (iii) annealed in Figs 3 and 4) whereas the NiO layer seems to become ordered, as deduced from the Ni 2p spectrum in which the double-peaked $2p_{1/2}$ band is now better resolved. This effect can be explained in terms of the heat of formation of both oxides, i.e. NiO and CuO.[3]

CONCLUSIONS

Quantitative chemical XPS analysis of the data is consistent with a Stranski–Krastanov growth mode, i.e. the formation of a first (3 Å) Ni monolayer followed by the formation of defective NiO islands 30–40 Å high. By comparing these results with the oxidation kinetics of bulk Ni, we conclude that the presence of the Cu substrate inhibits the oxidation of Ni. Further Ni deposition in an oxygen atmosphere leads to coalescence of the islands and the formation of stoichiometric NiO. At this stage of growth, the Cu substrate is also oxidized to CuO at the interface. Further annealing of the layer up to 400 °C produces reordering of the layer and reduction of the Cu^{2+} to metallic Cu.

Acknowledgements

This work has been supported financially by the DGICYT of Spain through contract number PB96-0061 and by the EU-TMR programme under contract ERBFMGECT 950063 at LURE. We also thank the staff of LURE for technical support.

REFERENCES

1. Vurens GH, Salmerón M, Somorjai GA. *Prog. Surf. Sci.* 1990; **32**: 333.
2. Henrich VE. *Prog. Surf. Sci.* 1995; **50**: 77.
3. Henrich VE, Cox PA. *The Surface Science of Metal Oxides*. Cambridge University Press: Cambridge, 1994.
4. Fujimori A, Minami F. *Phys. Rev. B* 1984; **30**: 957.
5. Sawatzky GA, Allen JW. *Phys. Rev. Lett.* 1984; **53**: 2339.
6. McKay JM, Henrich VE. *Phys. Rev. B* 1985; **32**: 6764.
7. Veenendaal MA, Sawatzky GA. *Phys. Rev. Lett.* 1993; **70**: 2459.
8. Soriano L, Abbate M, Vogel J, Fuggle JC, Fernández A, González-Elipe AR, Sacchi M, Sanz JM. *Chem. Phys. Lett.* 1993; **208**: 460.
9. Soriano L, Abbate M, Fernández A, González-Elipe AR, Sirotti F, Rossi G, Sanz JM. *Chem. Phys. Lett.* 1997; **266**: 184.
10. Alders D, Voogt FC, Hibma T, Sawatzky GA. *Phys. Rev. B* 1996; **54**: 7716.
11. Sanz JM, Tyuliev G. *Surf. Sci.* 1996; **367**: 196.
12. Kishi K, Hayakawa Y, Fujiwara K. *Surf. Sci.* 1996; **356**: 171.
13. Fuentes GG, Soriano L, Morant C, Trigo JF, Quirós C, Sanz JM, to be published.
14. Onsgaard J, Bjørn JA. *J. Vac. Sci. Technol. A* 1993; **11**: 2179.
15. Daas den H, Gizeman OLJ, Geus JW. *Surf. Sci.* 1993; **285**: 15.

16. Tougaard S, Hansen HS. *Surf. Interface Anal.* 1989; **14**: 730.
17. Tougaard S. *Surf. Interface Anal.* 1998; **26**: 249.
18. Tanuma S, Powell CJ, Penn DR. *Surf. Interface Anal.* 1991; **17**: 927.
19. Abbate M, Goedkoop JB, De Groot FMF, Grioni M, Fuggle JC, Hofmann S, Petersen H, Sacchi M. *Surf. Interface Anal.* 1992; **18**: 65.
20. Cheang-Wong JC, Ortega C, Siejka J, Ortiz C, Sacchi M, Carniato S, Dufour G, Rochet F, Roulet H. *Appl. Surf. Sci.* 1993; **64**: 313.
21. Kishi K, Fujita T. *Surf. Sci.* 1990; **227**: 107.
22. Mitchell DF, Sewell PB, Cohen M. *Surf. Sci.* 1976; **61**: 355.
23. Tougaard S. *J. Vac. Sci. Technol. A* 1990; **8**: 2197.
24. Tougaard S, Hetterich WH, Nielsen AH, Hansen HS. *Vacuum* 1990; **41**: 1583.
25. Fujita D, Schleberger M, Tougaard S. *Surf. Sci.* 1995; **331–333**: 343.
26. Schleberger M, Fujita D, Tougaard S. *Surf. Sci.* 1995; **331–333**: 942.
27. Tougaard S, Hansen HS. *Surf. Sci.* 1990; **236**: 271.
28. Hansen HS, Tougaard S, Biebuyck H. *J. Electron Spectrosc. Relat. Phenom.* 1992; **58**: 141.
29. Schleberger M, Fujita D, Scharfschwerdt C, Tougaard S. *J. Vac. Sci. Technol. B* 1995; **13**: 949.
30. Fink J, Müller-Heinzerling Th, Scheerer B, Speier W, Hillebrecht FU, Fuggle JC, Zaanen J, Sawatzky GA. *Phys. Rev. B* 1985; **32**: 4899.
31. Grioni M, Goedkoop JB, Schoorl R, De Groot FMF, Fuggle JC, Schäfers F, Koch EE, Rossi G, Esteva JM, Karnatak RC. *Phys. Rev. B* 1989; **39**: 1541.

